Supporting information for

Computational discovery of PtS_2/GaSe van der Waals heterostructure for solar energy applications

Rui Xiong[1], Rong Hu[1], Yinggan Zhang[2], Xuhui Yang[1], Peng Lin[1], Cuilian Wen[1], Baisheng Sa[1,*] and Zhimei Sun[3,**]

[1]*Key Laboratory of Eco-materials Advanced Technology, College of Materials Science and Engineering, Fuzhou University, Fuzhou 350108, P. R. China*

[2] *College of Materials, Fujian Provincial Key Laboratory of Theoretical and Computational Chemistry, Xiamen University, Xiamen 361005, P. R. China*

[3]*School of Materials Science and Engineering, and Center for Integrated Computational Materials Science, International Research Institute for Multidisciplinary Science, Beihang University, Beijing 100191, P. R. China*

*Corresponding Author: bssa@fzu.edu.cn (B. Sa).

**Corresponding Author: zmsun@buaa.edu.cn (Z. Sun).

Table S1. The parameters for the solar cell simulation

Materials properties	PtS_2/GaSe	CIGS	ZnO
Thickness [μm]	0.002	2	0.05
Bandgap [eV]	1.81	1.1	3.37
Electron affinity [eV]	4.4	4.5	4.6
Dielectric permittivity	5.2	13.6	9
Density of states in CB [cm^{-3}]	6.39×10^{18}	2.2×10^{18}	2.2×10^{18}
Density of states in VB [cm^{-3}]	2.52×10^{19}	1.8×10^{19}	1.8×10^{19}
Thermal velocity of electron [cm/s]	1.86×10^{7}	1×10^{7}	1×10^{7}
Thermal velocity of hole [cm/s]	1.17×10^{7}	1×10^{7}	1×10^{7}
Electron mobility [$cm^2/(V\ s)$]	3168	100	150
Hole mobility [$cm^2/(V\ s)$]	2188	25	25
Donor concentration [cm^{-3}]	1×10^{19}	0	1×10^{17}
Acceptor concentration [cm^{-3}]	0	2×10^{16}	0
Absorption coefficient [cm^{-1}]	file	SCAPS	SCAPS
Radiative recombination coefficient [cm^{-3}/s]	1.0×10^{-10}	1.0×10^{-10}	1.0×10^{-10}

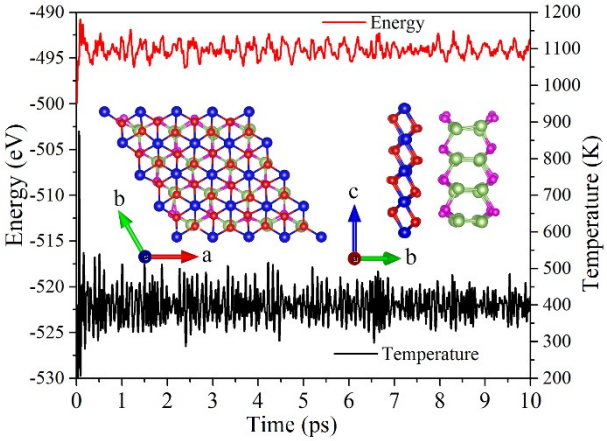

Figure S1. Evolution of total energy and temperature as well as snapshot structure from AIMD simulations of PtS_2/GaSe heterostructure.

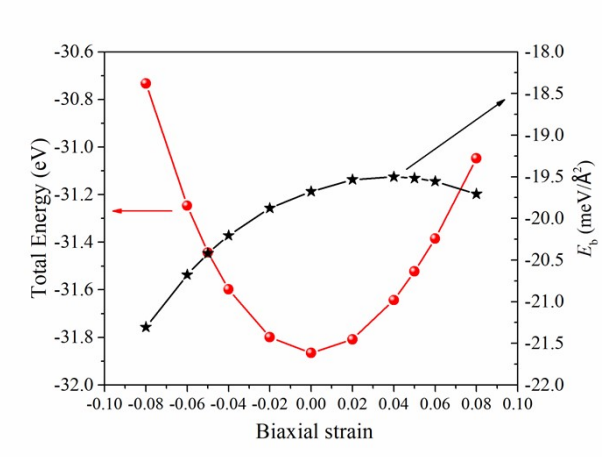

Figure S2. The total energy and binding energy (E_b) of PtS_2/GaSe heterostructures as function of biaxial strain.

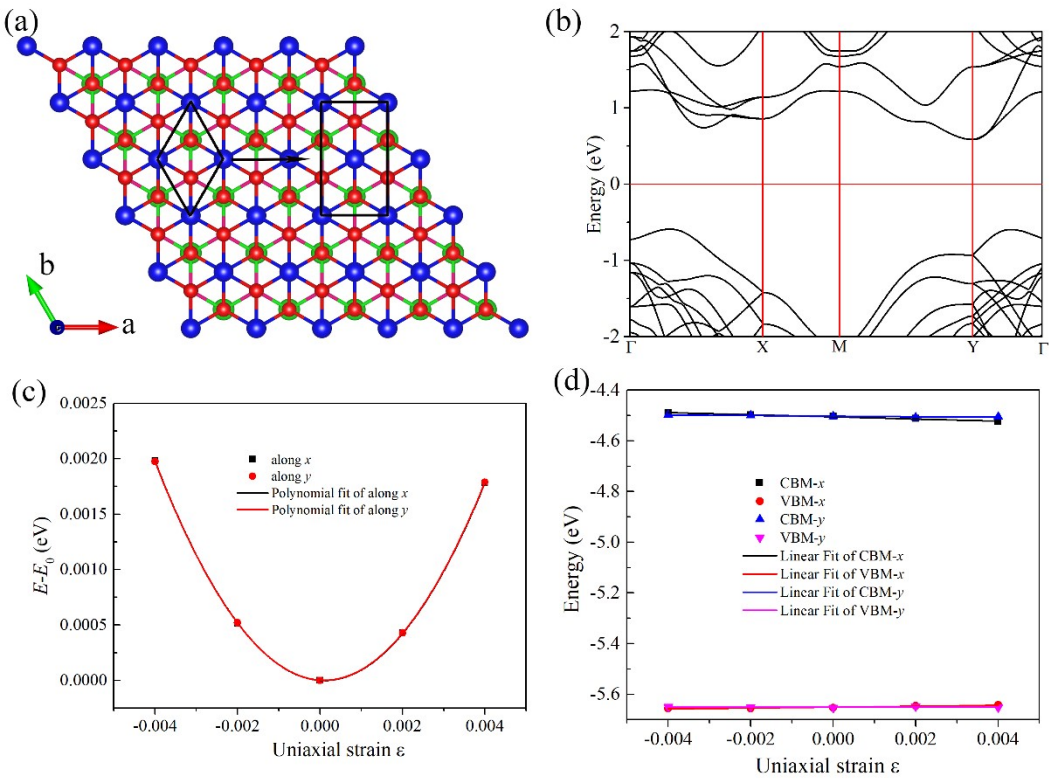

Figure S3. (a) The orthorhombic lattice structure and (b) band structure of PtS_2/GaSe heterostructure. (c) Total energy shift ($E - E_0$) and (d) band edge positions of PtS_2/GaSe as a function of the uniaxial strain ε along both the zigzag (x) and armchair (y) directions by using PBE functional.

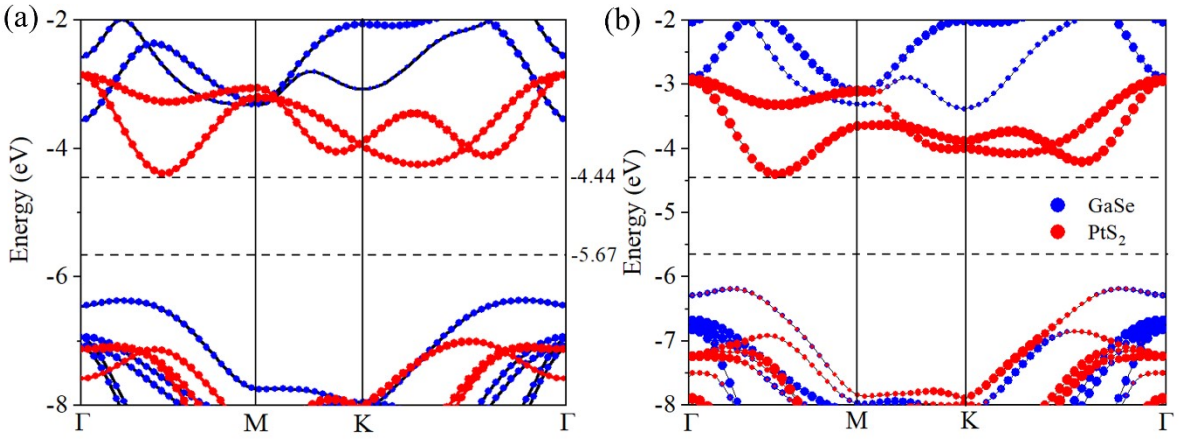

Figure S4. (a) The band structures of PtS_2 (red line) and GaSe (bule line) monolayers constrained in the PtS_2/GaSe heterostructure lattice constants based on the HSE06 functional. (b) Layered projected band structure of PtS_2/GaSe heterostructure, in which red and blue balls represent the contribution of up-layer (PtS_2) and down-layer (GaSe)

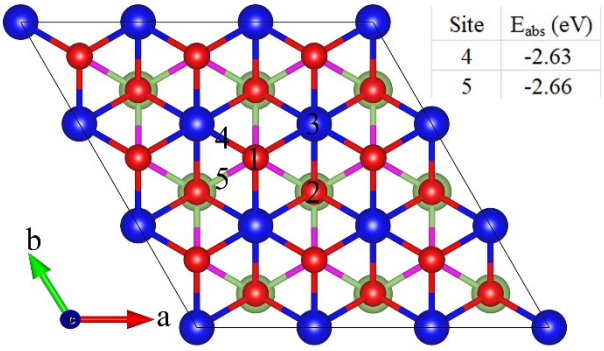

Figure S5. The possible absorption sites of H atom on the PtS_2 surface.

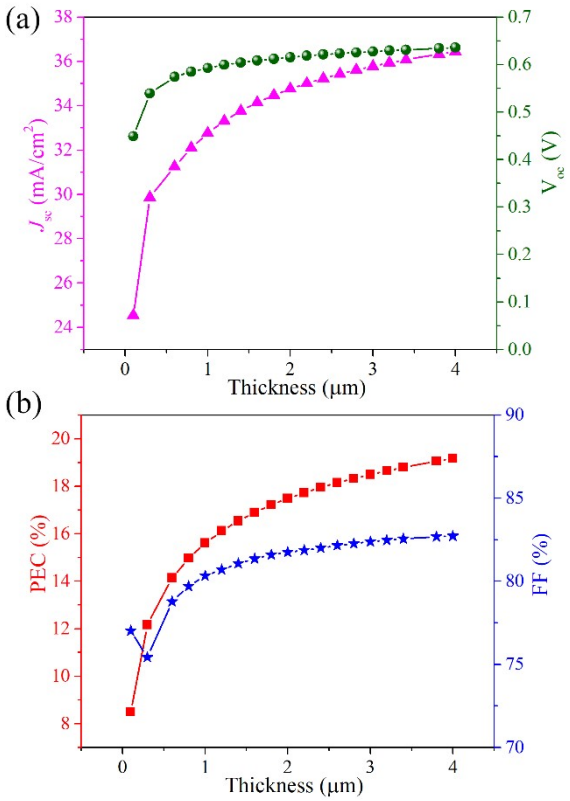

Figure S6 (a) The short-circuit current (J_{sc}) and open-circuit voltage (V_{oc}), (b) power efficiency conversion (PEC) and fill factor (FF) as function of CIGS thickness.

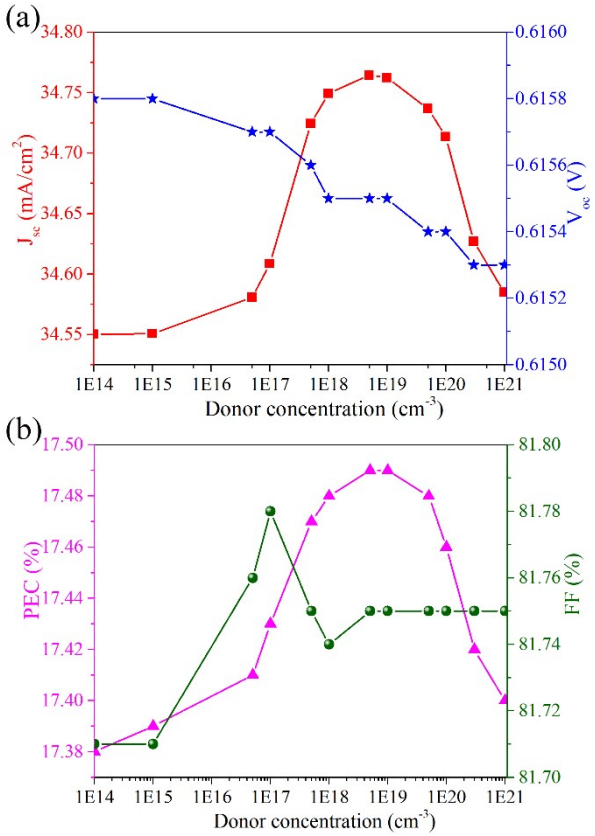

Figure S7 (a) The short-circuit current (J_{sc}) and open-circuit voltage (V_{oc}), (b) power efficiency conversion (PEC) and fill factor (FF) as function of PtS_2/GaSe carrier concentration.